Appl Phys B (2012) 109:477–483
DOI 10.1007/s00340-012-5060-3

Applied Physics B
Lasers and Optics

Chirped laser dispersion spectroscopy with harmonic detection of molecular spectra

M. Nikodem · D. Weidmann · G. Wysocki

Received: 10 February 2012 / Published online: 26 May 2012

Abstract Chirped laser dispersion spectroscopy (CLaDS) has been introduced recently as a technique that performs molecular detection based on measurement of optical dispersion. In this paper, a new detection scheme based on chirp modulation (CM) and subsequent phase-sensitive detection is described. CM-CLaDS inherits the full advantages of conventional CLaDS and additionally overcomes some of its limitations. A prototype CM-CLaDS instrument has been developed and characterized in laboratory conditions. The system is based on a distributed feedback quantum cascade laser which operates around 4.52 μm and can probe the most intense nitrous oxide (N_2O) ro-vibrational transitions. Preliminary performance tests are presented and provide a path/bandwidth normalized minimum N_2O detection limit below 100 ppbv m/Hz$^{1/2}$.

1 Introduction

Laser-based spectroscopy is an effective tool for selective molecular sensing that provides an excellent detection sensitivity and high temporal resolution. Most of the gas-sensing approaches that use optical techniques rely on probing of molecular or atomic absorption spectra. For low concentrations, the absorption is inherently small and the changes in the received optical intensity (due to absorption) can be several orders of magnitude smaller than the total power reaching a photodetector. This causes dynamic range and baseline issues that fundamentally limit the performance of direct absorption methods. Alternative techniques relying on absorption-induced secondary effects, such as photoacoustic spectroscopy or laser induced fluorescence can be baseline-free but are limited to specific system configurations. These methods would not be suitable for, for instance, long-distance open-path remote sensing.

Using molecular dispersion for trace gas sensing can overcome baseline and dynamic range limitations while still offering prospects for long range remote operation. Although the detection of refractive index changes in the vicinity of the molecular transition as a tool for molecular spectroscopy was studied a century ago [1] little progress has been made to date to adopt this approach to routine, sensitive trace-gas detection outside laboratory [2–10]. Recently we have introduced a chirped laser dispersion spectroscopy (CLaDS) technique in which information about the gas sample is retrieved from the measurement of the refractive index changes [11]. With CLaDS, the molecular dispersion signature is deduced from the frequency variation of the heterodyne beatnote between two waves that originate from a single frequency-chirped laser source. As the spectral information is encoded in the frequency of the beatnote, CLaDS is highly immune to optical power fluctuations, whilst maintaining sensitive molecular detection capabilities. The technique therefore offers prospect for long-distance open-path optical monitoring, where large variations in the received optical power can occur. Potential applications include environmental monitoring, remote sensing of hazardous gasses, fence line monitoring of emissions, or remote detection of leaks in gas pipelines. CLaDS immunity to power fluctuations offers the key advantage that allows overcoming issues related to changing environmental transmission (i.e. particu-

M. Nikodem · G. Wysocki (✉)
Electrical Engineering Department, Princeton University,
Princeton, NJ 08544, USA
e-mail: gwysocki@princeton.edu

D. Weidmann
Space Science and Technology Department,
STFC Rutherford Appleton Laboratory, Didcot OX11 0QX, UK

late matter or turbulence), hard target reflectivity variations, or pointing stability inaccuracies. Additionally, unlike absorption, refractive index changes are linear with molecular concentration hence CLaDS can provide an extended dynamic range of concentration measurements (from detection limit to concentration at which sample becomes almost opaque). In long open-path sensing this feature provides higher flexibility in optical path selection, because for optical path-lengths at which absorption lines would saturate the dispersion signal shows desirable linear dependence.

In our previous works we have demonstrated properties of CLaDS and some of its key advantages [11, 12]. In this paper an improvement to the original method is presented. We introduce a novel detection scheme that relies on chirp modulation (CM) and subsequent harmonic detection of the beatnote frequency. CM-CLaDS is shown to overcome some of the major limitations of conventional CLaDS. The first section summarizes the basics of the CLaDS approach. The following section describes the details of CM-CLaDS technique. Typical spectroscopic signals have been modeled and compared to experimental results. For experimental demonstration detection of nitrous oxide (N_2O) has been chosen based on its importance to environmental sensing. N_2O is one of the greenhouse gases with significant global warming potential [13] and the identification and quantification of its sources contributes to the understanding of the N_2O budget. The CM-CLaDS instrument is characterized in laboratory conditions and its application to molecular detection in ambient air is discussed.

2 Dispersion sensing using conventional CLaDS

Figure 1 shows the optical arrangement of conventional CLaDS. The laser beam from a chirped laser source passes through an acousto-optical modulator (AOM) driven with a sinusoidal waveform at frequency Ω. Part of the radiation is diffracted by the AOM (first order). The diffracted wave is frequency-shifted with respect to the incident laser radiation. The remaining part of radiation is transmitted through the AOM without frequency-shift as the 0th order beam. The two waves, the fundamental and the frequency-shifted one, are combined into a two-color laser beam that passes through the molecular sample and is focused onto a fast photodetector. The heterodyne signal produced by the beating of the two optical waves is frequency-demodulated at Ω by an RF spectrum analyzer. Due to the frequency difference between the two waves, as the laser frequency is chirped across a molecular transition, each wave experiences different phase velocities. As a result, molecular dispersion can be measured from the variation in the frequency of the heterodyne beatnote, which is obtained by FM-demodulation of the photodetector output signal (see Ref. [11] for details).

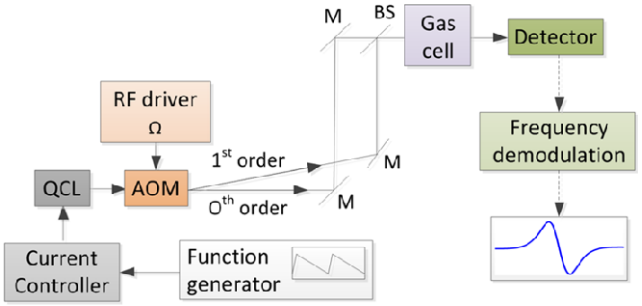

Fig. 1 Experimental arrangement of conventional CLaDS (*M*—mirror, *BS*—beam splitter)

Using a quantum cascade laser (QCL) or any other semiconductor laser as a source, the frequency chirp across a molecular transition can be produced by applying modulation to the injection current. After FM-demodulation of the photodetector signal the molecular content can be retrieved through fitting of the acquired conventional CLaDS spectrum with the dispersion profile calculated based on spectroscopic database. When absorption features are well reproduced by the Voigt profile, the dispersion spectrum can be efficiently calculated using the plasma dispersion function. For more complex lineshapes the dispersion spectrum can be obtained after the Kronig–Kramers transformation of the absorption coefficient.

Unfortunately, conventional CLaDS performance is impeded by two main limitations. First, the primary fundamental noise contribution stems from FM demodulation process. Due to a quadratic dependence of the FM-demodulation noise on the acquisition bandwidth, a trade-off between noise level and sampling resolution must be made [12]. Secondly, CLaDS is baseline-free only as long as the two frequency-shifted waves travel the same distance to the detector. In practice, however, maintaining this condition within sufficient level of accuracy without active opto-mechanical stabilization is challenging. As shown in Fig. 2, in some cases a path difference of only 1 mm might result in a baseline shift comparable to the amplitude of the target signal. Moreover, as the laser chirp is typically non-linear, the interferometer imbalance results in a non-linear baseline structure that requires fitting higher order polynomials for baseline correction. This makes the retrieval of concentration information less straightforward and may introduce additional signal processing artifacts.

3 Chirped Modulation CLaDS (CM-CLaDS)

CM-CLaDS has been developed to address the main limitations of conventional CLaDS, as discussed in the previous section. CM-CLaDS experimental arrangement is shown in Fig. 3. The laser chirp is modulated by a sinusoidal modulation of the laser injection current. Along with the CM,

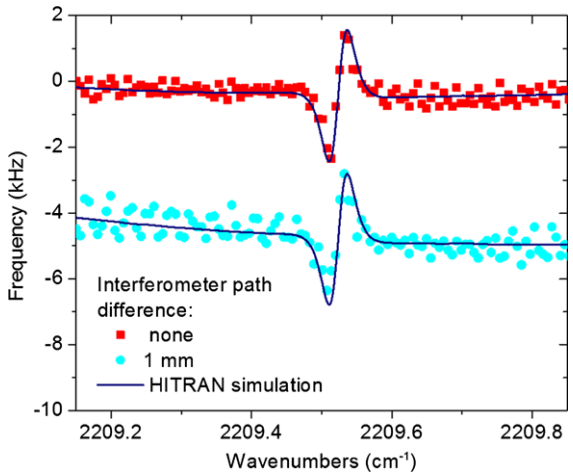

Fig. 2 Experimental dispersion spectra of the N_2O transition around 2209.5 cm^{-1} recorded using conventional CLaDS (*solid squares and circles*) and calculated dispersion profiles including a 2nd order polynomial baseline (*black solid lines*). The sample was 151 ppm of N_2O in N_2 placed in a 10-cm-long cell, with a total pressure of 300 Torr. The acquisition time was 1 s (10,000 scans averaged). The trace made of blue *solid circles* shows the impact of a 1 mm imbalance in the interferometer optical paths

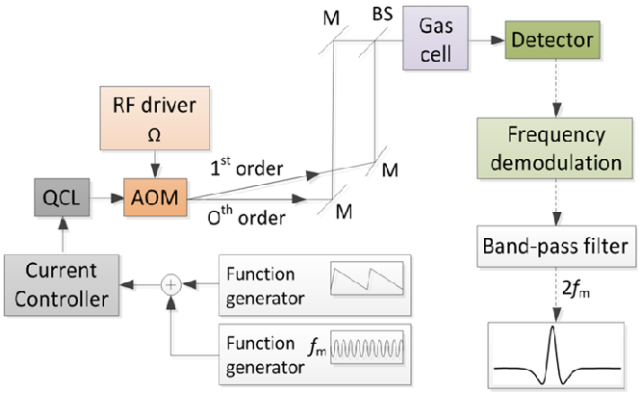

Fig. 3 Experimental arrangement of CM-CLaDS (*M*—mirror, *BS*—beam splitter)

a phase sensitive detection of the frequency demodulated signals is carried out to retrieve spectroscopic information. CM-CLaDS can be implemented either in a full dispersion spectrum acquisition mode (using an additional slow laser frequency sweep), or in a frequency-locked approach for direct continuous monitoring of concentration. In the line locked-mode the third harmonic of the demodulated dispersion signal is used as an error signal to actively lock the laser frequency on the peak of second harmonic signal.

In conventional CLaDS the signal is encoded as the instantaneous frequency of the heterodyne beatnote around carrier frequency Ω and is given by [11]:

$$f(\omega) = \frac{S}{2\pi c}\left[\Delta L - L_c\omega \cdot \left(\left.\frac{dn}{d\omega}\right|_{\omega-\Omega} - \left.\frac{dn}{d\omega}\right|_{\omega}\right)\right], \tag{1}$$

where S is the laser chirp rate, ΔL is path length difference between the interferometer arms, L_c is the path length within the gas sample, ω is the optical frequency and $n(\omega)$ is the optical frequency dependent refractive index of the medium. With CM-CLaDS, the chirp rate is modulated and can be expressed as

$$S = S_0 \sin(2\pi f_m t). \tag{2}$$

Therefore the instantaneous optical frequency becomes

$$\omega = \omega_0 + 2\pi \int S\,dt = \omega_0 + \omega_d \cos(2\pi f_m t), \tag{3}$$

where $\omega_d = 2\pi S_0/f_m$. By substituting (2) and (3) into (1) and assuming $\omega_0 \gg \omega_d$, the change of the FM demodulated instantaneous frequency of the heterodyne beatnote becomes

$$f(\omega_0, t) = \frac{S_0 \Delta L}{2\pi c}\sin(2\pi f_m t) - \frac{S_0 L_c \omega_0}{2\pi c}\sin(2\pi f_m t) \times \left(\left.\frac{dn}{d\omega}\right|_{\omega_0+\omega_d\cos(2\pi f_m t)-\Omega} - \left.\frac{dn}{d\omega}\right|_{\omega_0+\omega_d\cos(2\pi f_m t)}\right). \tag{4}$$

Subsequent phase-sensitive detection gives access to the Fourier coefficients for the in-phase and quadrature components of the FM-demodulated signal expressed by Eq. (4). Components of the nth harmonic are given by

$$a_n(\omega_0) = 2 f_m \int_0^{\frac{1}{f_m}} f(\omega_0, t)\cos(2n\pi f_m t)\,dt, \tag{5}$$

$$b_n(\omega_0) = 2 f_m \int_0^{\frac{1}{f_m}} f(\omega_0, t)\sin(2n\pi f_m t)\,dt. \tag{6}$$

With sinusoidal excitation all the a_n terms become zero. Since the first term in Eq. (4) is purely sinusoidal it will only contribute to the first harmonic (b_1). This term depends on the imbalance of the optical arms ΔL, which in consequence creates an unwanted baseline. Hence, by using higher harmonic detection ($n \geq 2$) the baseline contribution to b_n is fully suppressed even though imbalance still exists between the two frequency-shifted waves ($\Delta L \neq 0$).

This mathematical model has been implemented to produce numerical simulations of CM-CLaDS signals and a flow chart of the modeling steps is shown in Fig. 4. The lower part shows simulated signals for harmonics 1 through 6, using numerical integration as expressed by Eq. (6). It is obvious that the first harmonic does exhibit a strong baseline contribution that vanishes at higher harmonics. Because the signal amplitude decreases as the harmonic order increases, second harmonic detection offers the best trade-off in which baseline is fully suppressed while most of the signal amplitude is preserved.

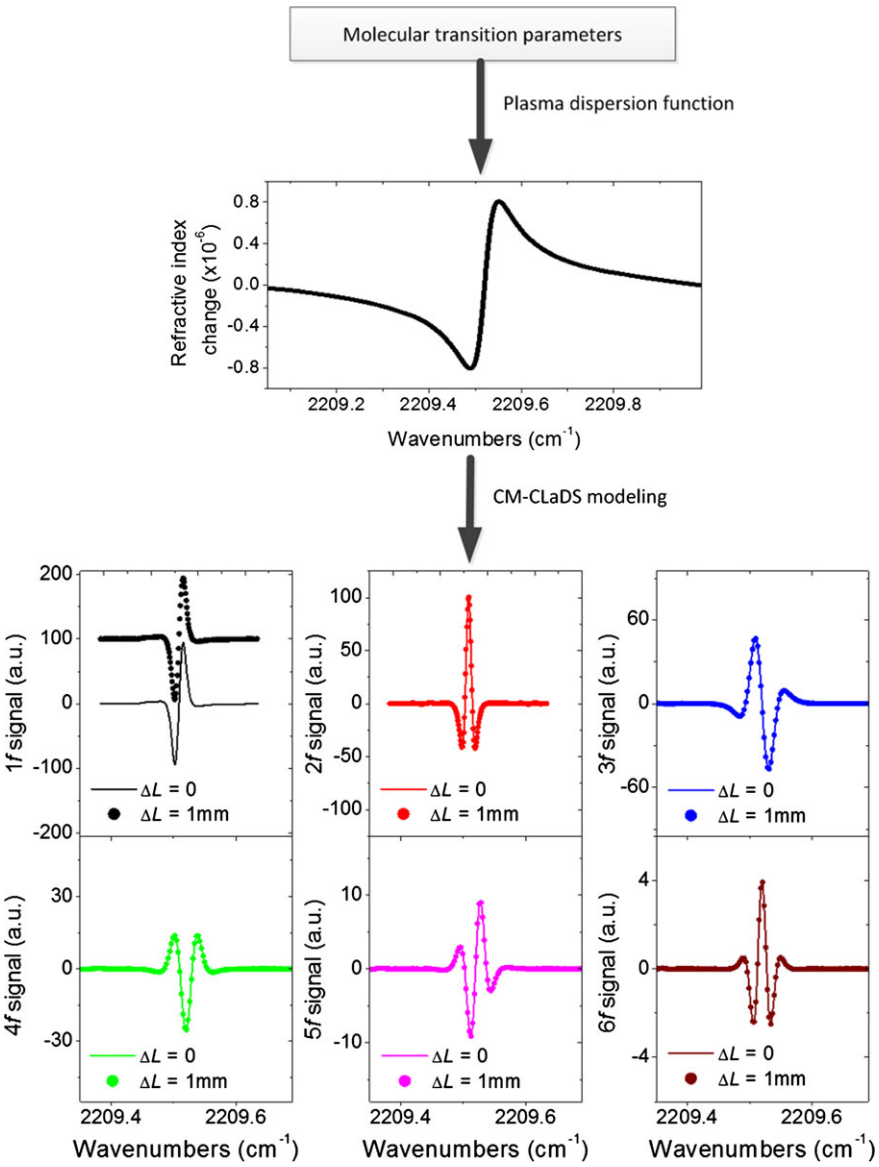

Fig. 4 A flow chart showing steps in simulating CM-CLaDS signals. Starting from spectral transition parameters (N_2O transition at 2209.52 cm^{-1}, taken from HITRAN), and sample parameters (total pressure of 100 Torr, $L_c = 0.1$ m, 150 ppm of N_2O in N_2), the dispersion profile is calculated using the plasma dispersion function. Then the CM-CLaDS model is used to numerically calculate the harmonic components

Not only does CM-CLaDS overcome the first limitation of conventional CLaDS (baseline), but it also addresses the issue of large FM noise contribution. Since in CM-CLaDS the acquisition bandwidth is greatly narrowed, the FM-noise is significantly reduced, which improves signal-to-noise ratio (SNR) of the instrument. The SNR at the output of the FM-demodulator is proportional to the square of the modulation index β, defined by [14]:

$$\beta = \frac{\Delta f}{f_m}, \tag{7}$$

where Δf is the maximal observed frequency deviation of the signal and f_m is the modulating frequency. In conventional CLaDS, the entire dispersion spectrum is the actual modulating signal, therefore large acquisition bandwidths (e.g. 10 MHz for spectra shown in Fig. 2) are required to capture the spectrum without distortion. As a result, the modulation index is low (typically in the range of 10^{-3} to 10^{-4}) which impedes the SNR. With the chirp modulation scheme the modulation is sinusoidal with a well-defined frequency. Thus the acquisition bandwidth can be narrower and the modulation index greater than in conventional CLaDS, hence allowing for higher SNR. Additional suppression of the FM-demodulation noise is carried out by a band-pass filter at the demodulator output centered at the selected harmonic of the modulation frequency.

4 Experimental demonstration of CM-CLaDS: N_2O sensing

The experimental demonstration of CM-CLaDS concept was carried out using a thermo-electrically (TE) cooled dis-

tributed feed-back (DFB) QCL (from Corning Inc.) operating at 4.52 μm, which enables access to the strongest fundamental ro-vibrational band of N_2O. The QCL was operated at 10 deg C in CW mode and provided approximately 5 mW of output power. The sample was contained in a 10-cm-long gas cell. We have used a TE cooled fast photodetector (Vigo Systems, PVI-3TE-10.6) to record heterodyne signal and an RF spectrum analyzer (Tektronix RSA6106A) to perform frequency demodulation. The laser frequency was chirped using a 100 kHz sinusoidal modulation added to the laser current and the $2f$ component of the frequency-demodulated signal was analyzed. A slow laser current ramp also provided to the chip was performing the frequency scan across the molecular transition. Optical fringing from the imperfectly AR-coated facets of the AOM was noticed in the system. The free-spectral range of the fringe pattern induced by the AOM was much smaller than the linewidth of the spectral features to be investigated, therefore they were effectively washed-out by applying a supplemental small frequency QCL current modulation at 1 kHz [15]. It should be noted that no baseline correction was performed in any of the experimental second harmonic dispersion spectra presented in the following sections.

4.1 Chirp modulation parameters

Sinusoidal chirp modulation in CM-CLaDS is achieved through modulation of laser frequency through injection current modulation. Although fundamentally different, such a signal generation/detection approach shows some similarities with wavelength modulation spectroscopy (WMS) technique [16]. For example, a careful choice of the modulation parameters is needed to achieve optimum SNR in both techniques. In WMS the modulation depth is optimized with respect to the width of the measured absorption line. In CM-CLaDS choosing the best modulation parameters is more complex. CLaDS signals are proportional to the chirp rate which is the time derivative of the wavelength modulation. Because the wavelength modulation depth of the chirp-modulating signal should be chosen to match the width of the probed dispersion profile, modulation of the laser frequency should be as fast as possible in order to increase the chirp rate and enhance CLaDS signal amplitude. Another complexity of CM-CLaDS with respect to WMS is related to dispersion profile width that depends not only on the sample pressure, but also on the frequency difference of the two superimposed waves. This must be taken into account in the optimization process.

The simulation algorithm presented in the previous section (Fig. 4) has been used to analyze and optimize these various parameters. Figure 5 shows the effect of modulation depth on the shape and amplitude of a $2f$ CM-CLaDS dispersion spectrum. The simulation parameters correspond

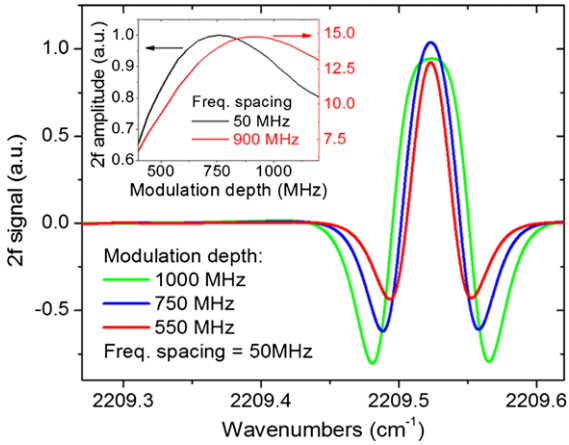

Fig. 5 Simulation of $2f$ CM-CLaDS spectra for different frequency modulation depths. The calculation was performed for a N_2O transition at 2209.5 cm^{-1}, 151 ppm of N_2O in N_2 at 300 Torr total pressure, and an AOM frequency of 50 MHz. The *inset* shows comparison of 2f CM-CLaDS peak signal amplitude as a function of modulation depth for 50 MHz and 900 MHz AOM frequency shift (the latter being optimal for these experimental conditions)

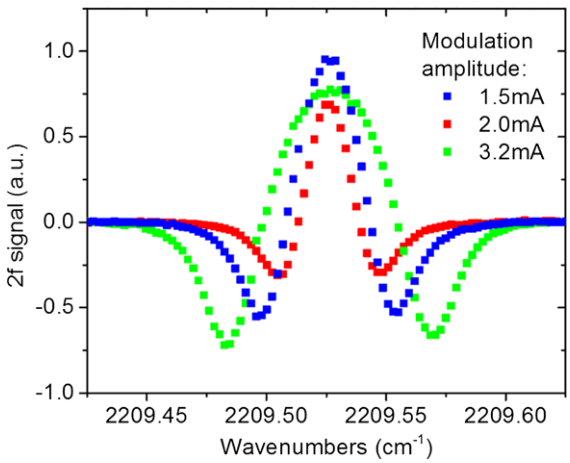

Fig. 6 $2f$ CM-CLaDS signals measured for different frequency modulation depths. Experimental conditions were identical to the parameters used in the simulations shown in Fig. 5

to those of the experimental demonstration shown in Fig. 6 (i.e. 50 MHz frequency spacing provided by the AOM, the N_2O transition at 2209.5 cm^{-1}, 10 cm long sample cell, and 151 ppm of N_2O in N_2 at a total pressure of 300 Torr). Inset in Fig. 5 also shows the CM-CLaDS signal amplitude vs. modulation depth for the optimal AOM frequency shift of $\Omega = 900$ MHz compared to $\Omega = 50$ MHz that was actually used in the experiment. The optimum frequency shift approximately corresponds to the linewidth of the dispersion profile, and yields significantly higher CLaDS signal amplitude (see Ref. [11] for details). The experimental results in Fig. 6 show good agreement with the simulation in Fig. 5.

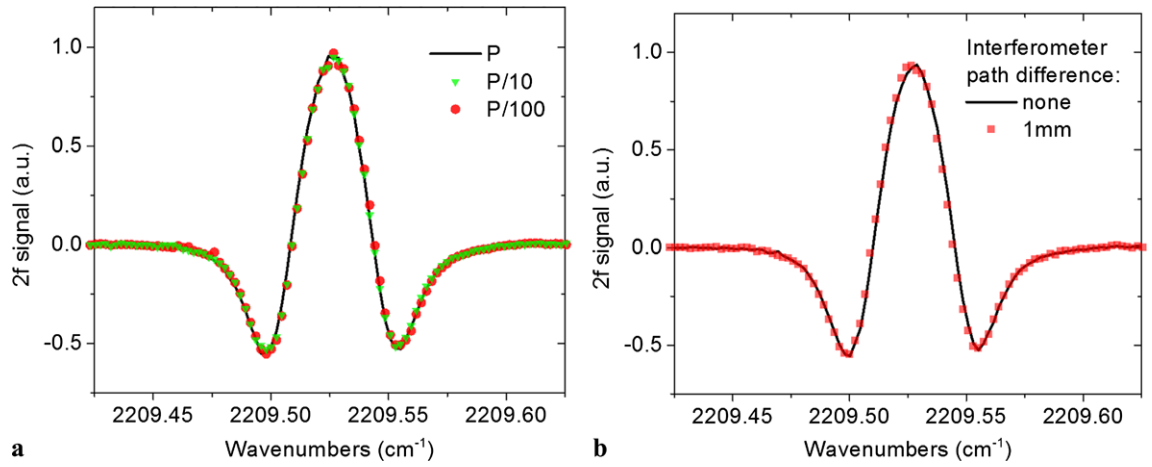

Fig. 7 2f CM-CLaDS dispersion spectra; (**a**) signals recorded for three different beatnote powers (−15, −25 and −35 dBm); (**b**) signals recorded with balanced and imbalanced ($\Delta L = 1$ mm) interferometer. Experimental conditions were identical to those given in Fig. 5

4.2 Immunity to optical power variations

One of the key properties of CLaDS is the high immunity of dispersion signals to changes in the optical power collected by the photodetector [11]. An analysis of the CLaDS SNR as a function of the received optical power was performed in Ref. [12]. This immunity also holds for CM-CLaDS. Evidence is shown in the experimental traces of Fig. 7a. Three spectra obtained at three different RF powers are shown to overlap perfectly (no dependence of CM-CLaDS signal amplitude on the received power). Moreover, despite a 20 dB change in RF signal power there is no noticeable deterioration in SNR.

4.3 Suppression of baseline effects

The theoretical baseline-free nature of the $2f$ CM-CLaDS signals has been highlighted in the previous section. The experimental validation has been carried out and is shown in Fig. 7b. For comparison, the experimental conditions are identical to the conventional CLaDS spectra presented in Fig. 2 where the $\Delta L = 1$ mm imbalance of the optical arms of the interferometer resulted in a large offset of the signal baseline. With $2f$ CM-CLaDS, despite similar ΔL, the spectrum is baseline-free.

4.4 Detection limit

As shown above, CM-CLaDS offers a robust immunity to baseline effects caused by $\Delta L \neq 0$. It should be noted that optical fringes represent an optical phase structure and can result in generation of parasitic CLaDS signal. However, if the spurious optical fringing is minimized (for example, through selection of system components such as AOM with well-designed AR-coatings), CLaDS can be considered free of any baseline effects. This creates the opportunity to use $2f$ CM-CLaDS system in a line-locked mode that actively sets the laser wavelength onto a desired transition and enables continuous monitoring of the gas sample concentration. Providing a calibration of the system has been performed, the $2f$ signal amplitude gives a direct measurement of the target gas concentration with no need of time-consuming spectral fitting. Moreover, contrary to WMS, CLaDS is immune to optical power fluctuations and power-normalization of detected signals becomes unnecessary [17–19].

To characterize the detection limit of the CM-CLaDS instrument in a line-locked mode, the laser wavelength was tuned to the center of N_2O line at 2209.52 cm^{-1} and the amplitude of the $2f$ CM-CLaDS signal was recorded. The maximal continuous acquisition time was limited to approximately 60 seconds due to hardware limitation of the RF spectrum analyzer. From the temporal record, Allan variance was calculated and is shown in Fig. 8 (black line). An averaging time of 1 s results in an SNR of ∼214, which corresponds to a minimum detection limit of 71 ppb m/$Hz^{1/2}$. To overcome the spectrum analyzer buffer size limitation and perform a stability test over a period longer than 1 minute, the data acquisition method had to be modified. The signal was acquired continuously for 50 ms with 1 s intervals between the consecutive acquisitions. The 950 ms between the acquisitions were needed for data processing. As a result, the duty cycle (and thus the effective integration time) has been reduced 20 times, but the system stability could be studied over longer periods. As shown in Fig. 8 (blue line) the instrument is stable up to hundreds of seconds before the system drift becomes dominant. Because of the duty cycle reduced by a factor of 20, the SNR was expected to drop by a factor of approximately $\sqrt{20}$ compared to the signal

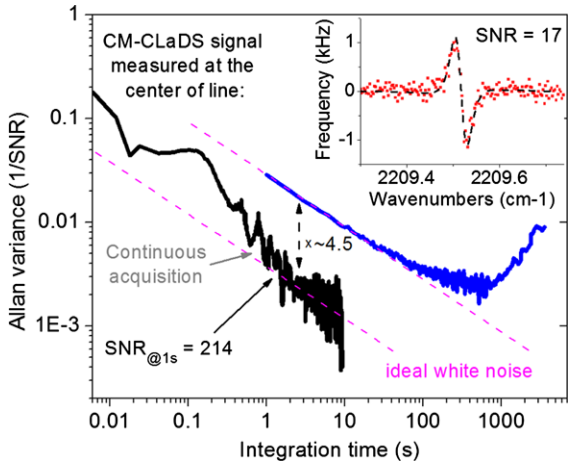

Fig. 8 The Allan variance analysis of CM-CLaDS system with the laser wavelength locked at the transition peak. Experimental conditions were identical to those given in Fig. 5. *Black*—continuous acquisition, *blue*—data acquired with 5 % duty cycle. *Inset*: signal recorded under the same conditions using a conventional CLaDS (*red dots*) showed together with the corresponding simulation (*black dotted line*)

acquired continuously. This is indeed observed in Fig. 8 as a ∼4.5 offset between the plotted curves.

To compare the detection sensitivity of CM-CLaDS with that obtained without CM, a conventional CLaDS trace was recorded under the same conditions and it is shown in the inset of Fig. 8. For this measurements the optical fringes induced by the AOM were suppressed by acquiring 10000 scans (100 μs/scan) while the AOM temperature was varied. This approach for fringe scrambling has been reported in Ref. [12]. Due to thermal expansion of the AOM crystal the free-spectral range of fringes changes, which enables efficient signal averaging with fringes significantly suppressed. Using this method, the SNR achieved by conventional CLaDS was 17, which yields a detection limit of only ~ 900 ppb m/Hz$^{1/2}$.

5 Conclusions

A novel detection scheme relevant to the chirped laser dispersion spectroscopy was introduced. CM-CLaDS is shown to overcome the major limitations of conventional CLaDS. The novel approach produces signals that are baseline-free even in the presence of opto-mechanical drift of the setup. This represents a significant improvement over the conventional CLaDS approach. Additionally, CM-CLaDS allows significant reduction of the RF detection bandwidth required to resolve the spectrum. As a result, the SNR can be improved by more than one order of magnitude compared to the non-CM version. Also, a small demodulation bandwidth required by CM-CLaDS facilitates application of low-cost electronics used in FM radio receivers for demodulation of the molecular dispersion signals from the heterodyne beatnote. CM-CLaDS was also shown to preserve the immunity of conventional CLaDS to variations in received optical power. If compared with standard absorption-based WMS techniques this property has the added benefit that power normalization of the detected CM-CLaDS signals becomes unnecessary. That makes the CM-CLaDS particularly suitable for open-path long-distance sensing applications where transmission fluctuations are likely to occur. The current CM-CLaDS instrument has demonstrated a minimum detection limit of 71 ppb m/Hz$^{1/2}$ for N_2O, and hence enables sub-ppbv sensitivity when optical paths of ∼100 meters are used. Further improvements are expected by using more efficient AR coatings on the AOM facets to reduce spurious etalon, and by incorporating a frequency shifter capable of larger (∼1 GHz) frequency shifts.

Acknowledgements The authors acknowledge the financial support by the NSF CAREER award CMMI-0954897 and partial support by the MIRTHE NSF Engineering Research Center. Dr. Chung-En Zah from Corning Inc. is acknowledged for providing a laser for this study.

References

1. R.W. Wood, Proc. R. Soc. Lond. **69**, 157 (1901)
2. A.B. Duval, A.I. McIntosh, J. Phys. D, Appl. Phys. **13**, 1617 (1980)
3. R. Gross, R. Chodzko, E. Turner, J. Coffer, IEEE J. Quantum Electron. **16**, 795 (1980)
4. O.E. Denchev, A.G. Zhiglinskii, N.S. Ryazanov, A.N. Samokhin, J. Appl. Spectrosc. **36**, 267 (1982)
5. S. Marchett, R. Simili, Opt. Commun. **249** (2005)
6. J.J. Moschella, R.C. Hazelton, M.D. Keitz, Rev. Sci. Instrum. **77**, 093108 (2006)
7. P. Werle, Spectrochim. Acta, Part A, Mol. Biomol. Spectrosc. **52**, 805 (1996)
8. A. Foltynowicz, W. Ma, O. Axner, Opt. Express **16**, 14689 (2008)
9. F.M. Schmidt, W. Ma, A. Foltynowicz, O. Axner, Appl. Phys. B, Lasers Opt. **101** (2010)
10. J. Mandon, G. Guelachvili, N. Picqué, Opt. Lett. **32** (2007)
11. G. Wysocki, D. Weidmann, Opt. Express **18**, 26123 (2010)
12. M. Nikodem, D. Weidmann, C. Smith, G. Wysocki, Opt. Express **20**, 644 (2012)
13. United States Environmental Protection Agency, "Methane and nitrous oxide emissions from natural sources" (April 2010). Available at www.epa.gov/nitrousoxide/sources.html
14. A.B. Carlson, P.B. Crilly, *Communication Systems: An Introduction to Signal and Noise in Electrical Communication* (McGraw-Hill, New Dehli, 2010)
15. D.T. Cassidy, J. Reid, Appl. Phys. B, Lasers Opt. **29**, 279 (1982)
16. P. Kluczynski, J. Gustafsson, Å. M. Lindberg, O. Axner, Spectrochim. Acta, Part B: Atom. Spectrosc. **56** (2001)
17. T. Fernholz, H. Teichert, V. Ebert, Appl. Phys. B, Lasers Opt. **75**, 229 (2002)
18. P. Kluczynski, O. Axner, Appl. Opt. **38**, 5803 (1999)
19. A. Farooq, J.B. Jeffries, R.K. Hanson, Appl. Opt. **48**, 6740 (2009)